Sound velocity and attenuation in bubbly gels measured by transmission experiments

Valentin Leroy,[a] Anatoliy Strybulevych, and John H. Page
Department of Physics and Astronomy, University of Manitoba, Winnipeg, Manitoba R3T 2N2, Canada

Martin G. Scanlon
Department of Food Science, University of Manitoba, Winnipeg, Manitoba R3T 2N2, Canada

Measurements of the phase velocity and attenuation of sound in concentrated samples of bubbly gels are presented. Hair gel was used as a matrix material to obtain well characterized distributions of bubbles. Ultrasonic measurements were conducted over a large range of frequencies, including the resonance frequencies of the bubbles. Surprisingly good agreement with Foldy's prediction was found, even for monodisperse samples at resonance frequencies, up to volume fraction of 1%. Beyond this concentration, the effects of high-order multiple scattering were observed. These results support the feasability of ultrasonic techniques to investigate the size distribution of bubbles in a weak gel or liquid. © *2008 Acoustical Society of America.* [DOI: 10.1121/1.2875420]

I. INTRODUCTION

It is well known that the presence of bubbles in a liquid has a tremendous impact on its acoustic properties. For example, the injection of air in water with a volume fraction of $\Phi = 0.4\%$ is enough to reduce the velocity of sound at low frequencies to roughly 0.2 mm/μs, a value which is even lower than the velocity of sound in the air that comprises the bubbles. This property, strange as it may seem, is well established[1] and has been thoroughly checked experimentally.[2–4] On the other hand, the behavior of ultrasonic velocity and attenuation at higher frequencies is still not fully understood. According to Foldy's model,[5] the effective wave vector k for a monodisperse population of bubbles is given by

$$k^2 = \left(\frac{\omega}{v} + i\frac{\alpha}{2}\right)^2 = \frac{\omega^2}{v_0^2} + 4\pi n f(\omega, r), \qquad (1)$$

where v_0 is the velocity of sound in the pure medium, n the number of bubbles per unit volume, and $f(\omega, r)$ the scattering function at angular frequency ω for a bubble of radius r. Figure 1 shows the attenuation α and phase velocity v in water for a 0.4% volume fraction of 100 μm radius bubbles, as calculated by Eq. (1). As the frequency gets close to the resonance frequency of the bubbles ($\simeq$30 kHz in this case), the dispersion and the attenuation dramatically increase. Few experiments have been done to check the validity of Foldy's expression around the resonances of bubbles. In 1957, Silberman[6] acquired data by measuring standing waves in pipes filled with bubbly water. Unfortunately, the method was not very accurate for high attenuation regimes, because the requisite standing waves could not develop. Only a rough estimation of the attenuation was possible and results exhibited a strong discrepancy with the model in the presence of resonant effects, *even at volume fractions as low as a few*

hundredths of 1%, as pointed out by Commander and Prosperetti.[7] More recently, Wilson *et al.* reported significant progress[4] by developing an impedance tube specifically designed for exploring the high attenuation regime in bubbly liquids. [8] They found good agreement with Foldy's model, but their bubbly liquids were very dilute (0.054% at most) and the exact distribution of the bubble radii was not known.

In contrast to the lack of experimental investigations on this subject, the number of theoretical discussions of Foldy's model is striking.[9–13] In 1961, Waterman and Truell[9] published a criterion for the validity of Foldy's equation, demonstrating that an improvement of the model was needed when resonant effects were to be considered. The failure of Foldy's model is usually attributed to its inability to take into account the coupling between bubbles. Indeed, in Eq. (1), the scattering function f is that of an individual bubble. When the response of the bubbles to the acoustic energy input is so strong that interactions between them cannot be neglected, f should be replaced by a "collective" scattering function F. Several authors, using different approaches to the problem, proposed expressions for this new scattering function.[10–13] But none of these corrections[14] to Foldy's model has been able to fit Silberman's historical data better than Foldy's original model.

The aim of the present paper is to fill the gap in reliable experimental data on the propagation of sound in a bubbly medium at frequencies close to the resonance frequency of the bubbles. Wilson's work[4] represented a significant advance on Silberman's experiments, but results for higher concentrations of bubbles ($\Phi > 0.1\%$) and for accurately known size distributions are critically needed. In Sec. II, we present the experimental setup we developed to produce well-characterized bubbly media, and to investigate their acoustic properties. Section III briefly introduces Foldy's model, and the correction proposed by Henyey.[12] Section IV is devoted to the results for four different samples, with volume fractions of bubbles ranging from 0.15% to 5%. These
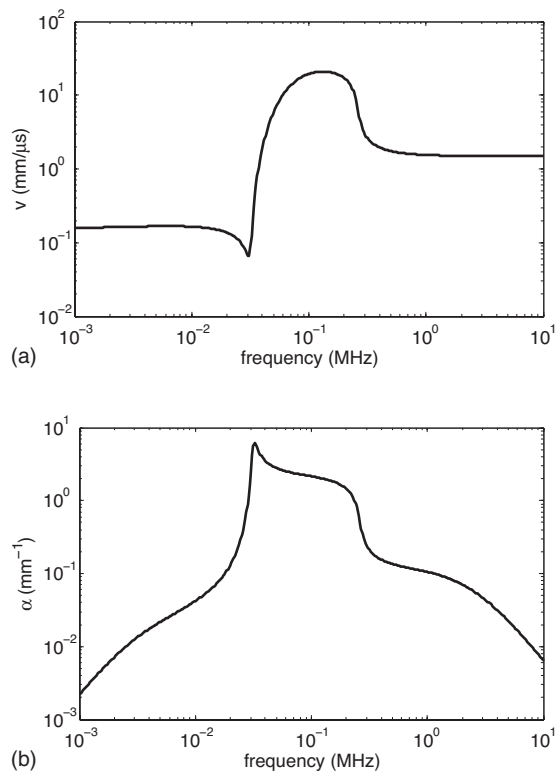
a)Electronic mail: valeroy77@yahoo.fr

FIG. 1. Prediction of Foldy's model for the phase velocity and attenuation of sound in water with a 0.4% volume fraction of 100-μm radius bubbles.

new results will be compared with Foldy's prediction, as well as with Henyey's model. Finally, Sec. V examines the conclusions that can be drawn from our analysis of these experiments.

It is worth noting that this question of knowing how sound propagates in a bubbly liquid when resonant effects are strong is not only of academic interest. From a practical point of view, acoustic methods are a very promising tool for investigating the size distribution of bubbles in a medium.[15,16] Since such methods rely precisely on the resonances of bubbles, a reliable model, valid for resonance frequencies, is necessary.

II. EXPERIMENTAL SETUP

To bring something new to the subject matter, experiments on propagation of sound in bubbly liquids have to satisfy three criteria: (1) Media with a range of bubble concentrations, going from very dilute to volume fractions of several percent, should be investigated; (2) the population of bubbles should be well characterized; and (3) the range of frequencies should include the resonance frequencies of the bubbles. With these stipulations, several experimental difficulties are apparent.

Standard techniques to measure the acoustic properties of a material involve propagating an acoustic pulse of short duration through a sample of the material. The time taken for each monochromatic wave component of the pulse to traverse the sample gives the phase velocity of sound in the material $v(\omega)$ [more precisely, $v(\omega)$ is the speed at which a surface of constant phase propagates at each frequency], and

the change in the wave amplitude gives the attenuation. In practice, a precise analysis with Fourier transforms is used, and comparison with propagation in a reference medium (usually water) is necessary. Such an experiment gives accurate measurements provided that the wavelength of the acoustic wave is small compared with two length scales: the lateral dimension of the sample, and the distance between the sample and the sound source. If this condition is not respected, diffraction and multiple reflections jeopardize the success of the technique. For bubbly liquids, this restriction has been a major impediment to experimental success. Indeed, the resonance of a bubble occurs at a very low frequency. As a rule of the thumb, a 1-mm-radius air bubble resonates in water at 3 kHz, which corresponds to a wavelength of 50 cm. Wilson et al. by-passed this difficulty by using the confined geometry of an impedance tube.[8] This solution necessitated the use of very thick stiff walls for the tube, so that the waves propagating in the tube were well approximated as plane waves. But the approximation is correct only for a narrow range of frequencies (specially designed to include the resonances of the bubbles in Wilson's case), and the use of thick walls makes in situ imaging of bubbles impossible. We used a different approach. As the resonance frequency of a bubble is inversely proportional to its radius, smaller bubbles make the experiment easier. In our samples, the bubble radius was typically 80 μm. The resonance frequency for bubbles of such a radius is 50 kHz, decreasing the wavelength to the more manageable scale of 3 cm.

A second experimental difficulty comes from the huge attenuation of sound in bubbly liquids. The consequence is that, in a transmission experiment, signals are of very small amplitude. A potential solution is to use a reflection configuration instead of a transmission one. But when the wavelength is large, so that it is not totally negligible compared with the dimensions of the setup, many complications arise in a reflection setup. Wilson et al. took advantage of their confined geometry to solve this problem. In our case, we used very thin samples, to ensure a sufficiently large signal in transmission despite the huge attenuation.

Finally, the question of obtaining a well-characterized medium is not a trivial one. Standard techniques of injection of gas in water, with needles and a pump or with an electrolysis device, are known to be capricious.[4,17] The production of bubbles is usually not repeatable from one experiment to the next or even during a single experiment. Moreover, the experimental sample cell is more difficult to design because a bubble generator has to be included. Our solution to this problem was to build stable samples of bubbly media by trapping bubbles in a gel whose yield stress was large enough to compensate for the buoyancy of the bubbles. This approach allowed us to work with samples whose bubble content was precisely known.

A. Sample preparation

A commercial hair gel,[18] diluted with water and degassed, was used as the liquid in which bubbles were injected. The benefit of hair gel for this experiment is that it
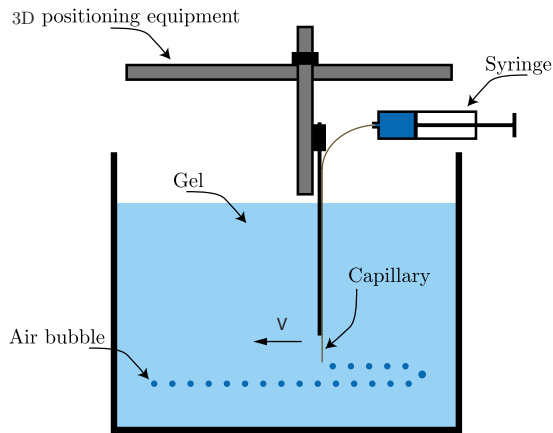
FIG. 2. (Color online) Injection of bubbles: A capillary is moved in a pre-programmed pattern of positions within the gel, delivering rows of equally sized bubbles. Capillary speed V and pressure in the syringe P are the two parameters governing the bubble size and the distance between bubbles.

flows only if the applied stress is larger than a threshold value (the yield stress). Hence if bubbles are sufficiently small, they remain trapped in the gel, at the exact place that they have been injected. In addition, from the acoustic point of view, the hair gel is very similar to water, at least for the frequencies considered in these experiments.

The samples were produced by a method developed in our laboratory and depicted in Fig. 2. A thin capillary (inner diameter of 20 μm), connected to a syringe with air at pressure P, is moved at constant speed V in the gel. With a well-controlled flow of gas through the capillary, as set by the pressure P, the movement generated an array of equally spaced bubbles of the same size. Although a discussion of the exact mechanisms involved in this process is outside the scope of this paper, we note that by varying the two parameters P and V, different bubble radii and distances between bubbles could be obtained. For our samples, we used a typical speed of $V=1$ cm/s and a pressure of $P=1.7$ bar, generating 80 μm bubbles separated by 500 μm. Thanks to a three-dimensional displacement stage, the vertical and lateral distance between successive rows of bubbles could be pre-programmed, depending on the desired total concentration. Once enough bubbles had been created, a sample of the bubbly medium was extracted with a syringe and injected into the cell designed for the ultrasonic device. Note that this last stage destroyed the ordered state of the bubbly medium. Future work is underway to investigate the acoustic properties of these crystals of bubbles. However, in the framework of an experimental test of Foldy's model, random collections of bubbles were needed. An important issue is the stability of the sample: If the degassed gel was undersaturated with air, bubbles dissolved in a matter of minutes. To prevent this, an interval of several days was required between the degassing of the gel and the injection, so that the hair gel was saturated.

Once the cell was filled with the bubbly gel and sealed, it was placed on a light box and images of the bubbles were taken with a digital camera connected to a microscope (2× magnification). Figure 3 shows examples of images taken for samples 2 and 3. The quality and contrast of the images were excellent, allowing an estimation of the diameter of the
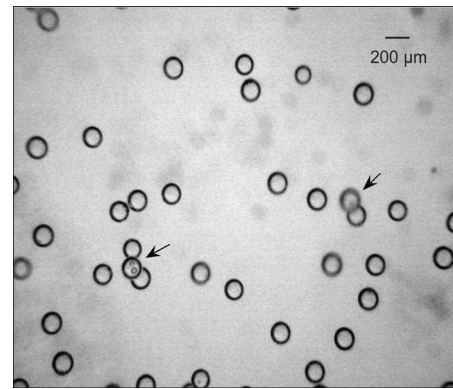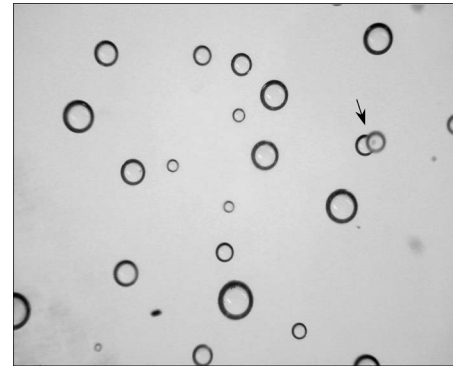
FIG. 3. Images of Sample 2 (monodisperse with *a* median radius of 86 μm) and Sample 3 (polydisperse). Arrows indicate clusters of bubbles ignored for the image analysis of the samples. The scale is the same on both images. Note that the dark spots in the background are not bubbles but dust on the back wall of the cell.

bubbles, with a resolution better than 2 pixels, by measuring the outer diameter of the dark ring appearing in the bubbles. Given the resolution of the images (438 pixels/mm), the uncertainty in the radii measurements was thus 2 μm. A dozen images, acquired at different positions within the samples, were analyzed with the "analyze particle" function of NIH IMAGEJ.[19] Furthermore, to check that the size of the bubbles remained stable during the experiment, images were taken both before and after the ultrasonic measurements. No significant evolution was noted. To avoid biased measurements of big bubbles, overlayed bubbles (such as the one marked with arrows in Fig. 3) were excluded from the size analysis. However, those bubbles were counted for the determination of the void fraction. Because the depth of field ($>$3 mm) was larger than the thickness of the cell (1.01 mm), the volume of one image was known and the number of bubbles per unit volume could be precisely determined (note that the darker grey marks in the background of the left image in Fig. 3 are not bubbles but are likely dust or dirt on the back wall of the cell). The resulting distributions $n(r)$ of radii r, as shown in Fig. 4, were well fitted by a lognormal distribution:

$$n(r) = \frac{n_{\text{tot}}}{\sqrt{2\pi}\epsilon r} \exp\left[-\frac{(\ln r/r_0)^2}{2\epsilon^2} \right], \quad (2)$$

with a median radius r_0, a logarithmic standard deviation ϵ, and a total number of bubbles per unit volume of n_{tot}. Un-
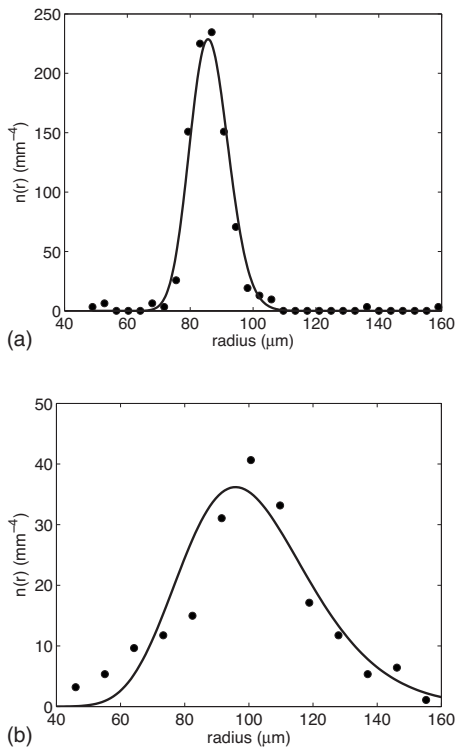
FIG. 4. Measured radius distributions for Samples 2 (top) and 3 (bottom) and best-fitted lognormal distributions.

certainty in volume fraction was estimated from the uncertainty in the radius measurement and uncertainty in the thickness of the cell.

The results of the image analysis procedure for the four samples we are presenting in this paper are given in Table I. The main parameter we varied was the volume fraction Φ, which ranged from 0.15% to almost 5%. Samples 1, 2, and 4 were very monodisperse. Sample 3 was obtained by letting Sample 2 evolve for 24 h. On this long time scale, there is a clear evolution of the size distribution: Larger bubbles grew at the expense of the smaller ones due to their different Laplace pressures, a process called Ostwald ripening.[20] The distribution of bubbles became polydisperse, as is evident from Fig. 3. Interestingly, the total volume fraction of air remained almost constant, indicating that the main mechanism of radius evolution was indeed ripening. Note that testing Foldy's model on a polydisperse sample is crucial for the goal of developing an acoustic bubble counting and sizing technique.

B. Ultrasonic measurements

The acoustic properties of the samples were measured with the setup of Fig. 5. In a large tank $(60 \times 60$

TABLE I. Measured parameters of the bubble size distributions for each sample. The number N of bubbles counted for the size analysis is indicated.

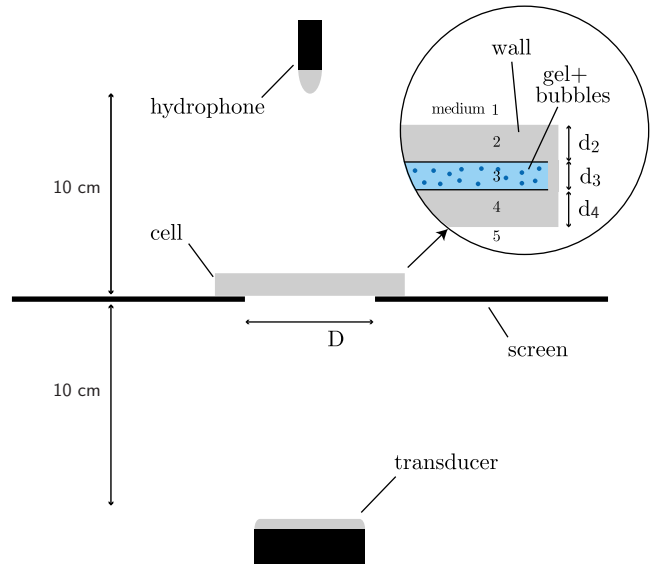| Sample	N	Φ	r_0	ϵ
1	50	$0.15 \pm 0.01\%$	$81 \pm 2 \ \mu m$	0.05 ± 0.01
2	288	$0.94 \pm 0.06\%$	$86 \pm 2 \ \mu m$	0.07 ± 0.01
3	186	$0.91 \pm 0.05\%$	$100 \pm 2 \ \mu m$	0.2 ± 0.02
4	141	$4.9 \pm 0.3\%$	$80 \pm 2 \ \mu m$	0.08 ± 0.01

FIG. 5. (Color online) Sketch of the setup for ultrasonic measurements. A piezoelectric transducer emits an acoustic pulse that traverses the cell containing the bubbly medium.

$\times 120 \ cm^3$) filled with reverse osmosis water, a piezoelectric transducer generated a pulse that propagated through water, traversed the sample, and reached the hydrophone. The amplitude of the acoustic signal was small enough ($\sim 10^3$ Pa) to prevent nonlinear response of the bubbles. Because the attenuation in the sample was large, and because the divergence of the beam was not negligible (especially at low frequencies), the use of a screen (a plastic ring wrapped with Teflon™ tape) was essential for reducing spurious signals. The aperture, D, of the screen had to be larger than the wavelength of the pulse, to limit diffraction effects, but smaller than the diameter of the cell. In our experiments, D was 6 cm, the cell diameter was 7 cm, and the maximum wavelength was 5 cm (for the lowest frequency of 30 kHz).

Gaussian pulses, with central frequencies ranging from 30 to 400 kHz, were generated by an Arbitrary Wave Generator, and two different transducers, having central frequencies of 100 and 250 kHz, were used to cover the range of frequencies. The pulses were recorded, with a hydrophone, in two different cases: when the cell was mounted on the screen $[s_1(t)]$, and when the cell was absent $[s_2(t)]$. The signals were averaged over 100 acquisitions when the attenuation was low (for reference measurements, for example), and up to 5000 acquisitions for highly attenuated signals. Signals $s_1(t)$ and $s_2(t)$ were then Fourier transformed into $S_1(\omega)$ and $S_1(\omega)$, respectively, and $x(\omega)$, the ratio of the transmission with and without the cell in the path of the acoustic beam at a given angular frequency, was calculated.

The data processing was complicated by the multilayer aspect of the cell. Indeed, the pulse did not propagate only through the bubbly medium but through five media (see Fig. 5): water (1), plastic (2), sample (3), plastic (4), and water again (5). Following Brekhovskikh,[21] when a plane monochromatic wave $\exp(ikx - i\omega t)$ propagates through the multilayered cell, it results in a transmitted plane wave $T \exp(ikx - i\omega t)$, where the complex transmission T is given by

Leroy *et al.*: Velocity and attenuation in bubbly gels

$d=d_3=1.01 \pm 0.05$ mm
$d_2=d_4=1.63 \pm 0.01$ mm
Velocity in walls: 2.28 ± 0.01 mm/μs
Density of walls: 1.19 ± 0.05g/cm^3

$$T = T_{54}T_{43}T_{32}T_{21}$$
$$= \frac{Z_4^{in} + Z_4}{Z_4^{in} + Z_5} e^{ik_4 d_4} \frac{Z_3^{in} + Z_3}{Z_3^{in} + Z_4} e^{ik_3 d_3} \frac{Z_2^{in} + Z_2}{Z_2^{in} + Z_3} e^{ik_2 d_2} \frac{2Z_1}{Z_1 + Z_2}, \quad (3)$$

where d_i is the thickness of layer i, $Z_i = \rho_i \omega / k_i$, k_i stands for the impedance and the wave vector in medium i respectively, and Z_i^{in} is the input impedance, which is given by

$$Z_i^{in} = \frac{Z_{i-1}^{in} - iZ_i \tan(k_i d_i)}{Z_i - iZ_{i-1}^{in} \tan(k_i d_i)} Z_i \quad \text{for } i > 1. \quad (4)$$

The unknown quantity in Eq. (3) is k_3. In the following, index 3 will be omitted: $d = d_3$, $k = k_3$. The ratio $x(\omega)$ is related to T by

$$x = T(k) e^{-ik_5(d_4 + d + d_2)}. \quad (5)$$

As $T(k)$ is a complicated function, inversion of Eq. (5) to extract k is not analytically possible. Note that the complication not only arises from the multiple reflections existing within the system, but also from the huge attenuation of sound in the bubbly medium. Indeed, as α and v are large, the wave vector in the sample $k = \omega/v + i\alpha/2$ has a non-negligible imaginary part. It follows that the phase shift of the pulse traversing the sample is not only due to propagation (as in standard cases) but also to the crossing of the interfaces 4-3 and 3-2. In other words, one cannot consider that the phase of the pulse is only dictated by the velocity in the sample, and that the amplitude of the pulse is only related to attenuation, which is a good approximation only when the term $\exp(ikd)$ dominates in Eq. (3). To address this issue, an iterative method can be set up. Let us define $\tilde{T}$ such that $T = \tilde{T} e^{ikd}$. Equation (5) can then be expressed as

$$e^{ikd} = x e^{ik_5(d_4+d+d_2)}/\tilde{T}(k), \quad (6)$$

and with Eq. (6) we can define the iteration:

$$k^{[j+1]} = -\frac{i}{d} \ln(x e^{ik_5(d_4+d+d_2)}/\tilde{T}(k^{[j]})). \quad (7)$$

The iteration can be initialized with $k^{[0]} = \omega/v_0$. It was tested with other initial values of $k^{[0]}$ and found to converge to the same final values of k even when the starting values were quite far from the final ones, indicating the robustness of the iteration procedure. Parameters of the cell are given in Table II. The uncertainty of the calculated wave vector k was evaluated by taking into account the uncertainty in the parameters (see Table II). It is worth noting that our experimental setup is adapted only for measurements in hugely attenuating materials. Filling the cell with water to measure the velocity of sound in water, for example, does not yield very

accurate results (namely, the precision is 0.5 mm/μs). The reason for this is that fully developed multiple reflections, as they exist when the cell is thin compared with the wavelength, make the inversion technique very sensitive to the exact parameters of the walls (density, velocity of sound, thickness). But when attenuation is large, the influence of multiple reflection within the cell is less pronounced, and reliable results can be obtained using a sufficiently thin sample that the transmitted pulse is of measurable amplitude.

III. THEORY

In this section we give a brief description of the two models that are compared with our experimental results. Equation (1) of Foldy's original model needs to be generalized to the polydisperse case:

$$k^2 = \frac{\omega^2}{v_0^2} + \int 4\pi n(r) dr f(\omega, r). \quad (8)$$

The scattering function at angular frequency ω for a bubble of radius r is given by

$$f(\omega, r) = \frac{r}{(\omega_0/\omega)^2 - 1 + i(\delta^{the} + \delta^{vis} + \delta^{rad})}, \quad (9)$$

where ω_0 is the resonance frequency of the bubbles and the three δ terms are the damping constants due to thermal, viscous, and radiative losses, respectively. A detailed model of the thermodynamic behavior of the oscillating bubble is due to Prosperetti.[23] A complex polytropic index can be defined as a function of the radius and the frequency:

$$\kappa(\omega, r) = \frac{\gamma}{1 - 3(\gamma - 1)i \frac{D_{th}}{\omega r^2} \mathcal{B}}, \quad (10a)$$

with

$$\mathcal{B} = 1 - \sqrt{-i} r \sqrt{\frac{\omega}{D_{th}}} \coth\left(\sqrt{-i} r \sqrt{\frac{\omega}{D_{th}}}\right), \quad (10b)$$

where γ is the ratio of specific heat capacities for air, D_{th} the thermal diffusivity of air, and where $\sqrt{-i}$ stands for $e^{i(3\pi/4)}$. Moreover, because our bubbles are in a gel, we also include the effect of the shear modulus, following Alekseev and Rybak.[24] The resonance angular frequency and the damping constants are then:

$$\omega_0^2 = \frac{3 \operatorname{Re}(\kappa)(P_0 + 2A/r) + 4\mu'}{\rho r^2} - \frac{2A}{\rho r^3}, \quad (10c)$$

$$\delta^{rad} = rk_0, \quad \delta^{the} = \frac{3 \operatorname{Im}(\kappa)P_0}{\rho r^2 \omega^2}, \quad \delta^{vis} = \frac{4\mu''}{\rho r^2 \omega^2}, \quad (10d)$$

where $k_0 = \omega/v_0$ is the wave vector in the gel, $\mu = \mu' + i\mu''$ the shear modulus of the gel, A its surface tension, ρ its density, and P_0 the ambient pressure. Values of the physical parameters we used for evaluating the equations are given in Table III. For the surface tension of the gel, we assumed it to be the same value as for water, which is probably an overestimation. In any case, surface tension effects are almost negligible for the bubble size considered in our experiments. Es-

J. Acoust. Soc. Am., Vol. 123, No. 4, April 2008

Leroy et al.: Velocity and attenuation in bubbly gels   1935

TABLE III. Values of the physical parameters used for the model. The phase velocity of sound in the gel was measured by propagating an acoustic pulse through a known thickness of gel. Shear moduli were obtained by standard rheological techniques. Density was measured with a specific gravity bottle.

$v_0 = 1.49$ mm/μs	$D_{th} = 2 \times 10^{-5}$ m^2/s
$\gamma = 1.4$	$P_0 = 10^5$ Pa
$A = 70$ mJ/m^2	$\rho = 1$ g/cm^3
$\mu' = 60$ Pa$(\omega/2\pi\text{Hz})^{0.1}$	
$\mu'' = 13$ Pa$(\omega/2\pi\text{Hz})^{0.5}$	

timation of the shear modulus was obtained via standard measurements with a rheometer, which gave the frequency dependence of μ up to 100 Hz. Extrapolation of this frequency dependence to 400 kHz is certainly a crude approximation. However, as μ' remains small compared with atmospheric pressure, its influence on the resonance frequencies of bubbles is weak [see Eq. (10c)], a fact that we experimentally checked by measuring the resonance frequency of individual bubbles in gel. Moreover, because thermal and radiative losses dominate, the effect of μ'' is not crucial: It changes, by 20% at most, the maximum of the attenuation of sound in the bubbly medium. As a result, the acoustic behavior of the bubbly gel is expected to be almost identical to what it would be for bubbly water.

In 1999, Henyey proposed a diagrammatic approach for the problem of propagation in a bubbly medium.[12] His result has a simple interpretation: It amounts to considering that the bubble does not radiate in the pure liquid, but in the effective medium. As a consequence, the radiative damping term in Eq. (10d) has to be modified, namely, k_0 in the formula of δ^{rad} has to be substituted by the effective wave vector k. We calculated Henyey's predictions by an iterative process, with 20 iterations. Note that Kargl, in 2002, obtained the same expression as Henyey, but with a different approach to the problem.[13]

IV. EXPERIMENTAL RESULTS

We present the experimental measurements of the attenuation and the phase velocity in four different samples of bubbly gels, with the parameters that characterize the bubble size distributions being given in Table I. For each sample, a comparison with Foldy's and Henyey's predictions is performed.

A. Low volume fraction

The first sample we investigated had a volume fraction of 0.15% with a monodisperse distribution of bubbles. Figure 6 compares an example of the pulse transmitted through the sample with the reference pulse through water, for a Gaussian pulse centered at 50 kHz. To measure the phase velocity and attenuation as a function of frequency, the Fourier transforms of the signals were computed. Figure 7 shows the magnitude of the Fourier transforms (top plot) and the difference between the phase of the reference signal and the phase of the sample signal (bottom plot), as functions of frequency. The dispersive character of the bubbly medium is clearly visible: Both the magnitude and the phase changed
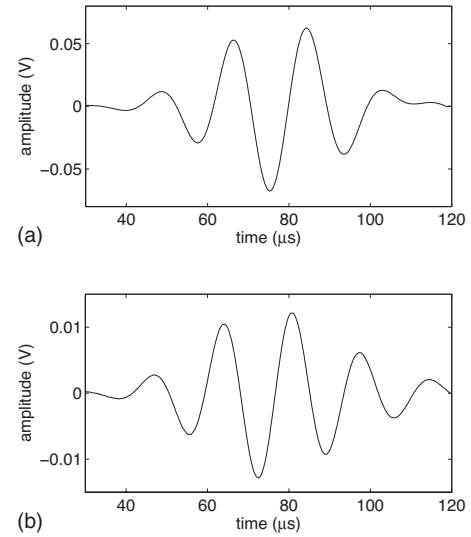

FIG. 6. Top: The reference pulse for a central frequency of 0.05 MHz. Bottom: The corresponding pulse transmitted through Sample 1.

significantly with frequency, particularly around 40 kHz, which is the resonance frequency of the bubbles.

From these calculations, the ratio x defined in Sec. II B was calculated and the attenuation and phase velocity were then determined using the procedure that was also described in this section (Sec. II B). Figure 8 displays the attenuation and velocity as a function of frequency for Sample 1. It is worth emphasizing that the entire regime of high attenuation is covered. For comparison, Wilson et al.[4] measured only the first part of the peak, and this was done for samples with a smaller concentration of bubbles. The error bars in the plots were calculated from the uncertainties in the different param-
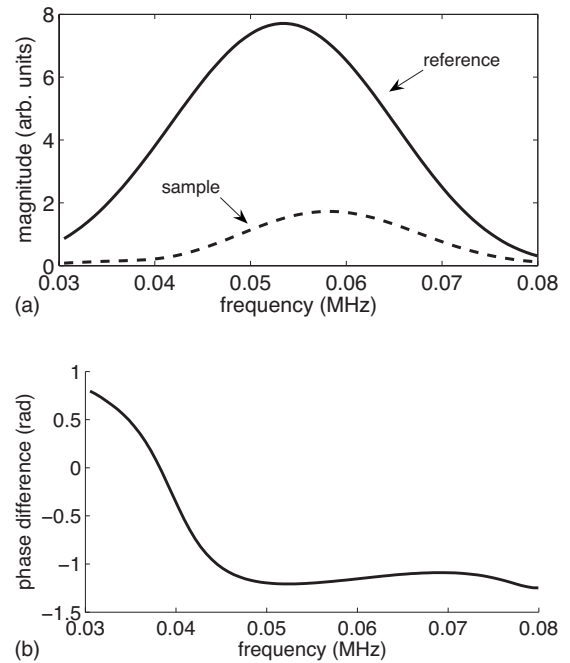

FIG. 7. Top: Magnitude of the Fourier transform of the reference signal of Fig. 6 (solid line) and of the sample signal of Fig. 6 (dashed line). Bottom: The phase of the Fourier transform of the reference signal minus the phase of the Fourier transform of the sample signal.
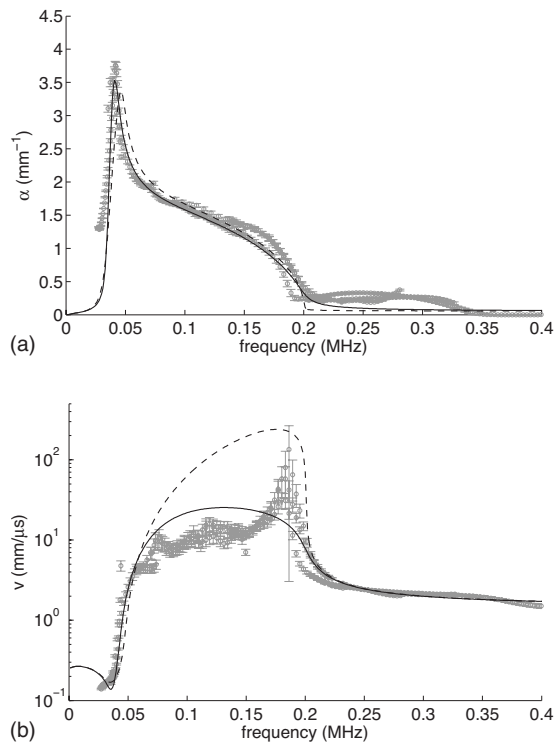
Leroy *et al.*: Velocity and attenuation in bubbly gels

FIG. 8. Attenuation and velocity measured in Sample 1 ($\Phi=0.15\%$, $r_0=81$ μm, $\epsilon=0.05$). Predictions from the Foldy (continuous lines) and Henyey (dashed lines) models are shown.

FIG. 9. Attenuation and velocity measured in Sample 2 ($\Phi=0.94\%$, $r_0=86$ μm, $\epsilon=0.07$). Predictions from the Foldy (continuous lines) and Henyey (dashed lines) models are shown.

eters needed for the inversion procedure (see Table II). Error bars are bigger when the phase velocity is large, because high values of velocity required measurement of small phase shifts. Note that the overlap in frequency between the different runs of data (with different Gaussian pulses) is satisfactory: One obtains more or less smooth curves. When differences are visible, they give indications about the uncertainty of the measurement.

Figure 8 also gives the predictions of Foldy's and Henyey's models for the bubble size distribution that was *measured in the sample*. In other words, there are no adjustable parameters in this treatment. For attenuation, there is good agreement with Foldy's model. A huge sharp peak of attenuation, due to resonance of the bubbles, is followed by a high attenuation regime (up to 200 kHz). The Henyey result (in dashed line) is not very different from Foldy's predictions for this sample, in which the concentration of bubbles is low. Nevertheless, the position of the attenuation peak is distinct from one model to the other, and Foldy's peak position is in better agreement with the measurements. Measurements of the velocity are more difficult to interpret. If only the rising and the decrease of the peak of velocity are examined, the agreement between Foldy's prediction and the experimental values is excellent. On the other hand, measurements from 100 to 200kHz display a large discrepancy with Foldy's model (note the logarithmic scale).

This discrepancy in the velocity may be a consequence of performing the experiments on well-characterized samples with fixed distributions of bubbles. Indeed, because our bubbles are trapped in the gel matrix—allowing us to take good 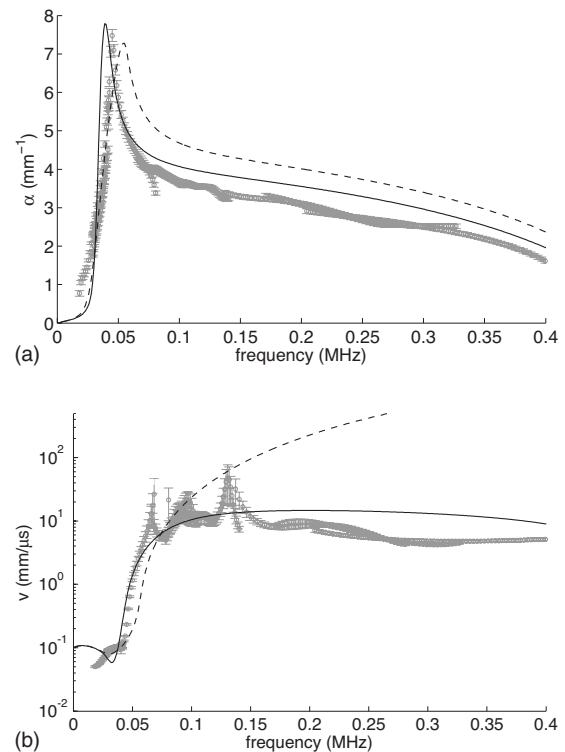and reliable images of them—our measurements are made with a particular realization, whereas the models calculate the properties of an average medium. In practice, it means that the signal acquired after passage through Sample 1 might be different from that measured through another sample with the same concentration of bubbles of the same size, but with bubbles in different positions. The signal obtained by averaging over the different configurations of the sample is usually called the coherent signal. The other part, which is related to a particular configuration, is called the incoherent signal. In our experiments, the incoherent part is expected to be very small, because the acoustic wavelength is so large compared with the typical distance between bubbles. It is therefore usually considered that the exact positions of the scatterers are not of crucial importance. However, a slight difference can exist and become non-negligible when one has to measure high values of α and v. Indeed, the relative magnitude of the incoherent part will increase as the coherent part is attenuated.[25] Furthermore, high velocities necessitate the measurement of small phase shifts, which may become blurred by the incoherent signal. This effect may explain the discrepancy between the models and our measurements of velocities larger than 10 mm/μs.

B. Intermediate volume fraction

The volume fraction of bubbles in Sample 2 was almost 1%. As displayed in Fig. 9, the measured attenuation shows a similar frequency dependence to that of Sample 1. The sharp peak of large attenuation is still at the same position (as expected, since the bubbles had the same radius), but of significantly larger magnitude. It is also apparent that the re-
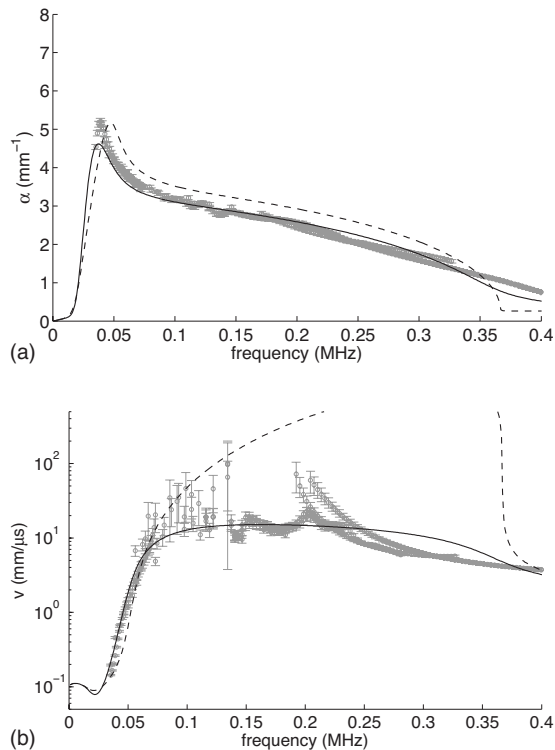
FIG. 10. Attenuation and velocity measured in Sample 3 ($\Phi=0.91\%$, $r_0 = 100$ μm, $\epsilon=0.2$). Predictions from the Foldy (continuous lines) and Henyey (dashed lines) models are shown.

FIG. 11. Top: The reference pulse for a central frequency of 0.25 MHz. Middle: The corresponding pulse traversing Sample 1 ($\Phi=0.15\%$, $r_0 = 81$ μm, $\epsilon=0.05$). Bottom: The corresponding pulse traversing Sample 4 ($\Phi=4.9\%$, $r_0=80$ μm, $\epsilon=0.08$). Note factor of 10^3 reduction in amplitude. Data in light grey correspond to the signal acquired when the aperture of the screen is closed.

gime of large attenuation is broader: α is still larger than 2 mm^{-1} at 0.4 MHz. The comparison with Foldy's prediction is not as good as for Sample 1. Although the magnitude of the sharp peak is well depicted, its position is not perfect. Furthermore, Foldy predicts an attenuation on the plateau which is 10% higher than what is measured. Henyey's model is in even worse agreement with the measurements. As for the velocity, its initial low frequency rise is well depicted by Foldy's model. On the other hand, above 100 kHz, agreement deteriorates, and Foldy's model predicts a larger velocity of sound than is found in the experiment. Velocity predictions from Henyey's model are in worse agreement.

C. Effect of polydispersity

Sample 3 had almost the same concentration of bubbles as Sample 2, but with a much more polydisperse distribution (see Fig. 4). Such well-defined samples provide a good opportunity to test the accuracy of ultrasonic measurements for obtaining details about the size distribution of bubbles in a sample. Comparison of Figs. 9 and 10 shows that a polydisperse sample can clearly be distinguished from a monodisperse one: The sharp peak in attenuation is shifted to a lower frequency and the general level of attenuation is substantially lower. The effect on velocity is less dramatic, the only clear difference being a less pronounced slope around bubble resonance for the polydisperse sample. All these features are well depicted by Foldy's model, which is again in better agreement with the experimental data than Henyey's model.
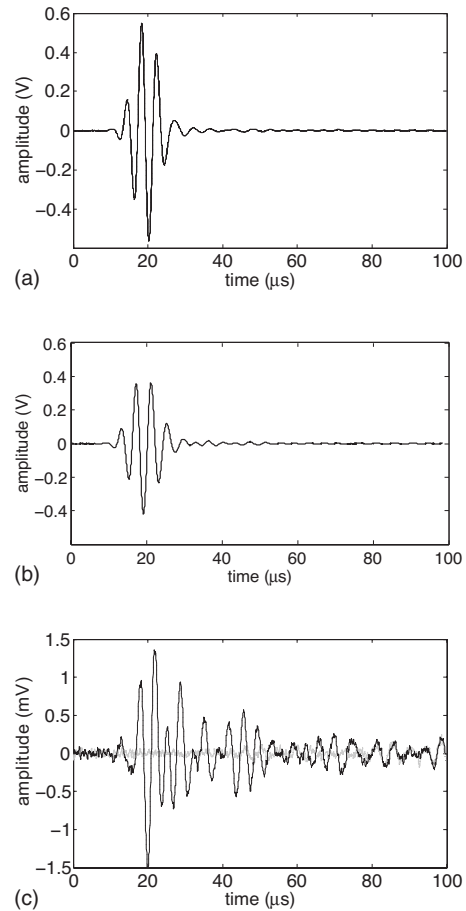
D. High concentration

With the high concentration (almost 5%) of monodisperse bubbles in Sample 4, we observed high-order multiple scattering. Figure 11 gives an example of the signal transmitted through Sample 4 (bottom plot) for a pulse of central frequency 0.25 MHz. For comparison, the pulses at the same frequency propagating through only water, as well as through Sample 1, are presented in Fig. 11 (top plot, and middle plot, respectively). It is clear from the top and bottom pulses in Fig. 11 that Sample 4 highly attenuates sound (by a factor 500), and also gives rise to high-order multiple scattering that is manifest as a tail of oscillations that follow the initial arrival of the signal.[25] By contrast, the pulses through the other samples, which have lower bubble concentrations, show no measurable signs of high-order multiple scattering (e.g., see the middle plot in Fig. 11). To check that this multiply scattered signal is due to the bubbly sample—and not to reflections in the water tank or around the screen—we also measured the transmitted signal when the aperture of the screen was closed (grey curve in Fig. 11). The pulse that has traveled through the bubbly medium is clearly much larger than this background signal, confirming the presence of high-
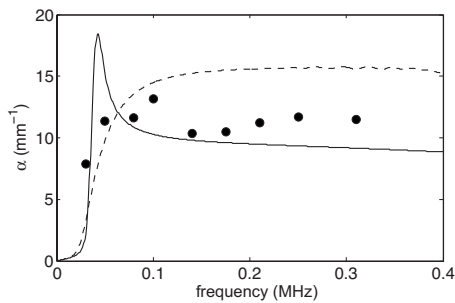
FIG. 12. Approximate measurements of the attenuation in Sample 4, and comparison with the Foldy (solid line) and Henyey (dashed line) models.

order multiple scattering and revealing that incoherent scattering is competing with the coherent field at this high concentration of bubbles.

For low frequencies, the presence of high-order multiple scattering was much less clear. Indeed, because the screen is less opaque to low frequency ultrasound, and because Sample 4 strongly attenuates the incident pulse, only the very first part of the acquired signal was different when the pulse was going through the sample or through the screen. We found that 0.15 MHz was the lowest frequency at which the existence of high-order multiple scattering could be clearly seen.

With a signal such as the one of Fig. 11, the analysis described in Sec. II B cannot be used because the coherent pulse cannot be clearly distinguished from the total measured field. However, a crude estimation of the attenuation can be performed by taking only the three first cycles of the signal, which likely consist mostly of the coherent component of the field, and by considering that the loss in transmission in Eq. (3) is dominated by $\exp(-\alpha d/2)$. The result of such a procedure is given in Fig. 12. The order of magnitude of the result is comparable to that of the theoretical models. But, due to the crudeness of the measurements, it is not possible to discern which model is better at predicting experimental results for samples with such high concentrations of bubbles.

V. CONCLUSIONS

We have measured the phase velocity and the attenuation in monodisperse bubbly media over a large range of frequencies that include the resonance frequency of the bubbles. For concentrations of 0.15% and 1%, we find that Foldy's model gives an imperfect but satisfactory description of the attenuation and phase velocity in our samples. In particular, the attenuation is well predicted by Foldy's model, but the phase velocity is overestimated for frequencies corresponding to the higher frequency part of the large attenuation regime. It is important to note that this range of frequencies over which the agreement between theory and experiment deteriorates *did not include the resonant frequencies of the bubbles.* This is a surprising result, as there is a general consensus in the literature about the inability of Foldy's model to describe the propagation of sound in a bubbly liquid *in the presence of resonant effects.* In that sense, our results confirm what Wilson *et al.*[4] obtained, but with

better characterized samples that contain higher concentrations of bubbles.

However, the question of knowing whether Foldy's model needs corrections or not, and what this correction should be, is still open. Indeed, our measurements with a small number of quenched samples did not allow us to unambiguously separate the coherent part of the signal from the incoherent scattering, even though each sample contained a large number of bubbles; thus, for this range of bubble concentrations, a definitive comparison of experimental data with theories for ensemble average properties, such as Foldy's or Henyey's models, must await additional experiments with a larger number of well-characterized samples. Also, our samples were thin, and, even though the samples were sufficiently dilute that significant short range correlations in the positions of the bubbles due the sample boundaries are unlikely, most of the bubbles were still near a boundary, and therefore may not have experienced the same effective field as in the idealized infinite sample assumed in the models. In future work, this question will be addressed through measurements on samples of different thickness, as has been done for other strongly scattering media, where the ability of effective medium theories to accurately describe velocity and attenuation data in thin samples has been demonstrated.[26,27] Despite the limited number of samples investigated in the current experiments, it is still interesting to note that better agreement with the data was found with Foldy's model than with Henyey's model.

Nevertheless, from a practical point of view, the results reported in this paper are encouraging for achieving the objective of measuring the bubble size distribution in a medium using ultrasonic techniques. In many such applications, the bubble sizes in a particular sample are needed. For concentrations of bubbles up to 1%, measuring the position, height, and shape of the peak of attenuation should give enough information to determine the distribution of bubble radii using Foldy's model. A demonstration of the feasibility of this approach was made with Samples 2 and 3, whose different polydispersity could be differentiated using attenuation measurements. Note that for higher volume fractions, when high-order multiple scattering is directly observable, it becomes more difficult to measure the velocity and attenuation; however, in this regime, useful information can still be obtained with techniques based on diffusing acoustic wave spectroscopy,[28,29] which can be applied to investigate the dynamics of the bubbles (e.g., Ostwald ripening) with excellent sensitivity.

[1]A. B. Wood, *A Textbook of Sound* (Bell, London, 1932).

[2]F. S. Crawford, "The hot chocolate effect," Am. J. Phys. **50**, 398–404 (1982).

[3]M. Nicholas, R. A. Roy, L. A. Crum, H. Oguz, and A. Prosperetti, "Sound emissions by a laboratory bubble cloud," J. Acoust. Soc. Am. **95**, 3171–3182 (1994).

[4]P. S. Wilson, R. A. Roy, and W. M. Carey, "Phase speed and attenuation in bubbly liquids inferred from impedance measurements near individual

bubble resonance frequency," J. Acoust. Soc. Am. **117**, 1895–1910 (2005).

[5]L. L. Foldy, "The multiple scattering of waves," Phys. Rev. **67**, 107–119 (1945).

[6]E. Silberman, "Sound velocity and attenuation in bubbly mixture measured in standing wave tubes," J. Acoust. Soc. Am. **29**, 925–933 (1957).

[7]K. W. Commander and A. Prosperetti, "Linear pressure waves in bubbly liquids: Comparison between theory and experiments," J. Acoust. Soc. Am. **85**, 732–746 (1989).

[8]P. S. Wilson, R. A. Roy, and W. M. Carey, "An improved water-filled impedance tube," J. Acoust. Soc. Am. **113**, 3245–3252 (2003).

[9]P. C. Waterman and R. Truell, "Multiple scattering of waves," J. Math. Phys. **2**, 512–537 (1961).

[10]C. Feuillade, "The attenuation and dispersion of sound in water containing multiply interacting bubbles," J. Acoust. Soc. Am. **99**, 3412–3430 (1996).

[11]Z. Ye and L. Ding, "Acoustic dispersion and attenuation relations in bubbly mixture," J. Acoust. Soc. Am. **98**, 1629–1635 (1995).

[12]F. S. Henyey, "Corrections to Foldy's effective medium theory for propagation in bubble clouds and other collections of very small scatterers," J. Acoust. Soc. Am. **105**, 2149–2154 (1999).

[13]S. G. Kargl, "Effective medium approach to linear acoustics in bubbly liquids," J. Acoust. Soc. Am. **111**, 168–173 (2002).

[14]Feuillade's model gives good agreement with experimental results, but it introduces an *ad hoc* adjustable parameter without a clear justification.

[15]R. Duraiswami and S. Prabhukumar, "Bubble counting using an inverse acoustic scattering method," J. Acoust. Soc. Am. **104**, 2699–2717 (1998).

[16]V. Leroy, Y. Fan, A. L. Strybulevych, G. G. Bellido, J. H. Page, and M. G. Scanlon, "Investigating the bubble size distribution in dough using ultrasound," in *Bubbles in Food 2: Novelty, Health and Luxury*, edited by G. M. Campbell, M. G. Scanlon, and D. L. Pyle (Eagan, St. Paul, MN, 2008).

[17]F. van der Biest, "Diffusion multiple et renversement du temps ultrasonore dans des milieux périodiques et désordonnés (multiple scattering and time reversal of acoustic waves in periodic and disordered media)," Ph. D. thesis, Université Paris 7, 2005.

[18]Dep, sport endurance gel, made in USA by Henkel corporation.

[19]M. D. Abramoff, P. J. Magelhaes, and S. J. Ram, "Image processing with image," Biophotonics Int. **11**, 36–42 (2004).

[20]R. Ettelaie, E. Dickinson, Z. Du, and B. S. Murray, "Disproportionation of clustered protein-stabilized bubbles at planar air-water interfaces," J. Colloid Interface Sci. **263**, 47–58 (2003).

[21]L. M. Brekhovskikh, *Waves in Layered Media* (Academic, New York, 1960).

[22]A. R. Selfridge, "Approximate material properties in isotropic materials," IEEE Trans. Sonics Ultrason. **SU-32**, 381–394 (1985).

[23]A. Prosperetti, "Thermal effects and damping mechanisms in the forced radial oscillations of gas bubbles in liquids," J. Acoust. Soc. Am. **61**, 17–27 (1977).

[24]V. N. Alekseev and S. A. Rybak, "Gas bubble oscillations in elastic media," Acoust. Phys. **45**, 535–540 (1999).

[25]Z. Q. Zhang, I. P. Jones, H. P. Schriemer, J. H. Page, D. Weitz, and P. Sheng, "Wave transport in random media: The ballistic to diffusive transition," Phys. Rev. E **60**, 4843–4850 (1999).

[26]J. H. Page, P. Sheng, H. P. Schriemer, I. Jones, X. Jing, and D. A. Weitz, "Group velocity in strongly scattering media," Science **271**, 634–637 (1996).

[27]M. L. Cowan, K. Beaty, J. H. Page, Z. Liu, and P. Sheng, "Group velocity of acoustic waves in strongly scattering media: Dependence on the volume fraction of scatterers," Phys. Rev. E **58**, 6626–6636 (1998).

[28]M. L. Cowan, J. H. Page, and D. A. Weitz, "Velocity fluctuations in fluidized suspensions probed by ultrasonic correlation spectroscopy," Phys. Rev. Lett. **85**, 453–456 (2000).

[29]M. L. Cowan, I. P. Jones, J. H. Page, and D. A. Weitz, "Diffusing acoustic wave spectroscopy," Phys. Rev. E **65**, 066605 (2002).